



Cite this: *RSC Adv.*, 2024, **14**, 27764

## A superporous and pH-sensitive hydrogel from *Salvia hispanica* (chia) seeds: stimuli responsiveness, on–off switching, and pharmaceutical applications

Maria Khatoon,<sup>a</sup> Arshad Ali,<sup>a</sup> Muhammad Ajaz Hussain,<sup>†</sup>  \*<sup>b</sup>  
 Muhammad Tahir Haseeb,<sup>c</sup> Muhammad Sher,<sup>a</sup> Omar A. Alsaidan,<sup>d</sup>  
 Gulzar Muhammad,<sup>e</sup> Syed Zajif Hussain,<sup>†</sup>  Irshad Hussain  f and Syed Nasir Abbas Bukhari<sup>g</sup>

The use of plant seed-based hydrogels to design drug delivery systems (DDSs) has increased due to their swellable, pH-responsive, biocompatible, biodegradable, and non-toxic nature. Herein, the chia seeds hydrogel (CSH) was extracted through an aqueous extraction method to explore its pH and salt-responsive swelling behavior and sustained release potential. The CSH was characterized using Fourier transform infrared (FT-IR) and solid-state cross-polarization magic angle spinning carbon-13 nuclear magnetic resonance (solid/state CP-MAS <sup>13</sup>C/NMR) spectra. Thermal analysis indicated that the CSH is a thermally stable material and decomposes in two steps. The scanning electron microscope (SEM) images of CSH witnessed the existence of microscopic channeling and a superporous nature with average pore sizes of  $18 \pm 11 \mu\text{m}$  (transverse cross-sections) and  $23 \pm 15 \mu\text{m}$  (longitudinal cross-sections). The CSH is a haemocompatible material. The CSH revealed pH and saline-responsive swelling in powder and compressed form (tablet) in the following order; distilled water (DW) > pH 7.4 > pH 6.8 > pH 1.2. Moreover, the swelling of CSH followed second-order kinetics. The swelling of CSH powder and tablets was decreased with increasing salt concentration. The pH, solvent, and saline responsive on/off switching (swelling/deswelling) results of the CSH and tablets disclosed its stimuli-responsive nature. The CSH prolonged the release of valsartan for 5 h at pH 7.4, whereas, negligible release (19.3%) was noted at pH 1.2. The valsartan release followed first-order kinetics and the non-Fickian diffusion. In conclusion, the CSH is a stimuli-responsive smart material with great potential to develop pH-sensitive and targeted DDSs.

Received 1st July 2024  
 Accepted 12th August 2024

DOI: 10.1039/d4ra04770b  
[rsc.li/rsc-advances](http://rsc.li/rsc-advances)

### 1. Introduction

*Salvia hispanica* (chia) is a famous angiosperm plant of the *Lamiaceae* (mint) family.<sup>1</sup> It is cultivated in the tropical and subtropical regions of Mexico and Guatemala, which are considered as the largest producer of chia, from where it is

exported to Japan, USA, and Europe.<sup>2</sup> Chia is utilized as a famous nutritional supplement. It is widely used in producing drinks, cereals, cookies, medicine, and foods.<sup>3</sup>

The chia seeds released polysaccharide-based hydrogel when soaked in water has been utilized as a good aid in the digestion of food.<sup>4</sup> The CSH contains high concentrations of uronic acid.<sup>5</sup> The polysaccharides present in the CSH consist mainly of glucuronic acid and xylose.<sup>6</sup> Advanced spectroscopic analyses have revealed the presence of  $\beta$ -D-xylopyranosyl and  $\alpha$ -D-glucuronopyranosyl units in the CSH.<sup>4</sup>

The CSH has shown various ecological functions including self-propagation, stability during the preparation of food products, and existence in tough environmental conditions.<sup>7,8</sup> Due to its exceptional ability to absorb and retain water, CSH has been used in the food industry as a thickening agent, preparation of emulsions, replacer of solid fat, texture forming, texture modifier agent, ice cream stabilizer, etc.<sup>9–11</sup> Some other relevant hydrogels from natural sources such as from the seeds

<sup>a</sup>Institute of Chemistry, University of Sargodha, Sargodha 40100, Pakistan

<sup>b</sup>Centre for Organic Chemistry, School of Chemistry, University of the Punjab, Lahore 54590, Pakistan. E-mail: [majaz172@yahoo.com](mailto:majaz172@yahoo.com); Tel: +923468614959

<sup>c</sup>College of Pharmacy, University of Sargodha, Sargodha 40100, Pakistan

<sup>d</sup>Department of Pharmaceutics, College of Pharmacy, Jouf University, Sakaka 72388, Aljouf, Saudi Arabia

<sup>e</sup>Department of Chemistry, Government College University Lahore, Lahore 54000, Pakistan

<sup>f</sup>Department of Chemistry, SBA School of Science & Engineering, Lahore University of Management Sciences, Lahore Cantt. 54792, Pakistan

<sup>g</sup>Department of Pharmaceutical Chemistry, College of Pharmacy, Jouf University, Sakaka, Aljouf, 72388, Saudi Arabia



of *Artemisia vulgaris*, *Cydonia oblonga*, and *Salvia spinosa*, etc.<sup>12-14</sup> are water-swellable, superabsorbent, porous, stimuli (pH, solvent, temperature, radiations, saline, etc.) responsive, non-toxic, non-thrombogenic, hemocompatible, and chemically modifiable materials. Such naturally occurring hydrogels have been extensively used to design benign DDSs, *i.e.*, tablets, injectables, dermal and transdermal gels, nasal gels, ophthalmic preparations, implants, etc., wound healing agents, tissue engineering materials, mucoadhesive preparations, nanogel, and water purification systems.<sup>15-18</sup> Furthermore, such hydrogels enhanced the release time of glucose, food, and drugs in the bloodstream.<sup>19,20</sup>

Green materials and sources are increasingly used in research instead of synthetic and semi-synthetic ones. Because plant-based materials are naturally abundant and mucilages isolated from plants are biocompatible, biodegradable, non-toxic, non-immunogenic, non-mutagenic, and economical, therefore scientists are increasingly focusing on using such natural materials, *i.e.*, mucilages/hydrogels in drug delivery systems. As a result, extensive research is currently being done on novel polysaccharide-based naturally occurring water-swellable materials, such as mucilage/hydrogels, which are extruded from seed coats, to explore their potential uses for stimuli-responsive drug delivery systems.

Hence, the current investigation aims at the hot water extraction of a polysaccharide-based mucilage (CSH) from chia seeds for novel pharmaceutical applications. The CSH and CSH-based novel tablet formulations will be analyzed through stimuli-responsive swelling studies at physiological pH, on-off switching in buffers, and salt solutions, and a smart material for drug delivery applications. The study being presented is an attempt to design a unique drug delivery system (smart tablets) using CSH, a smart polysaccharide-based biomaterial. Hence, we introduce a novel intelligent drug delivery system to target the intestines precisely. Additionally, we assess CSH's hemocompatibility for the first time using thrombogenicity and hemolysis investigations. The aim is also to characterize the CSH using FT-IR, solid/state CP-MAS <sup>13</sup>C/NMR, thermogravimetric analysis (TGA), and SEM analyses. We are keen to appraise the sustained release behavior of CSH-based tablet formulation at the pH of the small intestine.

## 2. Materials and methods

### 2.1. Materials

*Salvia hispanica* (chia) seeds were acquired from the local market of District Sargodha, Pakistan. A Botanist of the Department of Biological Sciences, University of Sargodha, Pakistan, verifies the taxonomy of the chia seeds. The chia seeds were manually cleaned, sieved, and stored in an air-tight jar at room temperature. The reagents and chemicals used in the research work were of analytical grade. The sodium chloride (NaCl,  $\geq 99\%$ ), potassium chloride (KCl,  $\geq 99\%$ ), sodium hydroxide (NaOH,  $\geq 98\%$ ), nitric acid (HNO<sub>3</sub>,  $\geq 65\%$ ), hydrochloric acid (HCl  $\geq 37\%$ ), and potassium dihydrogen phosphate (KH<sub>2</sub>PO<sub>4</sub>,  $\geq 99\%$ ), were procured by Riedel-de Haën, Germany. The *n*-hexane ( $\geq 95\%$ ), and ethanol (C<sub>2</sub>H<sub>5</sub>OH,  $\geq 98\%$ ), were of Sigma-Aldrich, USA. The microcrystalline cellulose (Avicel® PH

101), and tragacanth gum were of BDH (Bristol, England). The protocol as described in the United States Pharmacopeia-National Formulary (USP 34-NF 29) was used for the preparation of acidic (pH 1.2) and basic (pH 7.4) buffers. The drug (valsartan) was of USP standard and used as a model drug to evaluate the sustained release potential of CSH. Nylon mesh was used to isolate hydrogel from chia seeds. All the glassware was initially rinsed with HNO<sub>3</sub> and then washed with distilled water (DW). The DW was used to prepare necessary solutions and dilutions.

### 2.2. Isolation of hydrogel

The chia seeds were manually cleaned and soaked in DW for 12 h at room temperature and then heated at 60 °C for 1 h. The swollen seeds were placed over nylon mesh, squeezed, and rubbed with the help of a spatula to separate the hydrogel/mucilage from the seed coats. The isolated hydrogel, *i.e.*, CSH was collected in a beaker and initially washed with DW to make it free from polar impurities. Finally, the CSH was washed with *n*-hexane to remove non-polar and lipophilic impurities. After purification, the CSH was spread on a steel tray and put in an oven at 60 °C under vacuum to dry it. The dried CSH was stored in an air-tight container for further experimental work.

### 2.3. Characterization of CSH

The FT-IR spectrum of CSH was recorded after making its thin disc with KBr (CSH : KBr 2.5 : 97.5) under hydraulic pressure. The thin film of the sample was dried for an hour in a vacuum oven at 50 °C before analysis on an IR prestige-20 spectrophotometer (Shimadzu, Japan) in the range from 4000–400 cm<sup>-1</sup> with 20 scans and adjusting the resolution of 4 cm<sup>-1</sup>. The dried powder sample of CSH was run on solid-state cross-polarization magic angle spinning carbon-13 nuclear magnetic resonance (CP/MAS <sup>13</sup>C NMR) and the spectrum was recorded (100.4 MHz on a JEOL GX-400 spectrometer at 20 °C) through which the pattern of sugar was assessed.

The thermal stability of the CSH was determined through the record of its thermogravimetric (TG) curve and differential scanning calorimetry (DSC) heat flow thermograms using SDT Q600 thermal analyzer (TA Instruments, USA) from ambient temperature to 800 °C under a nitrogen environment. The heat flow was maintained at 100 cm<sup>3</sup> min<sup>-1</sup> at the onset heating rate of 15 °C min<sup>-1</sup>. Thermal data acquired was run on Universal Analysis 2000 version 4.2E (TA Instruments, USA), and MS Excel software was used to interpret the results.

The SEM micrographs of CSH were recorded on an SEM (FEI-NOVA, NanoSEM-450) equipped with an Everhardt-Thornley detector (ETD) to evaluate its surface morphology. For this purpose, the CSH (0.1 g) was first dried in a vacuum oven at 60 °C and imbibed in DW (50 mL). The swollen CSH was then sonicated for half an hour to remove air bubbles (if any). The sonicated sample was freeze-dried and then cut into transverse and longitudinal cross-sections with the help of a sharp blade. A sputter coater (Denton, Desk V HP) was used for coating the freeze-dried cross-sections of CSH with gold before recording the SEM micrographs at different magnifications. The



histograms were also drawn to determine the pore size of the internal structure of CSH. More than 150 positions for pore diameters were measured using ImageJ software and obtained data was processed to acquire the histogram of % frequency vs. pore diameter. Likewise, a similar procedure was used to observe the texture and cross-section area of the CSH-based tablets through the record of SEM micrographs.

#### 2.4. Flow-ability parameters of CSH

The ability of any material to be used as a pharmaceutical excipient depends on its ability to flow. Therefore, various flow-ability parameters including angle of repose ( $\theta$ ), bulk density ( $D_b$ ), tapped density ( $D_t$ ), Carr's index ( $C_i$ ), and Hausner ratio ( $H_r$ ) of CSH were determined to ascertain the flow properties of CSH as a pharmaceutical excipient.

**2.4.1. Angle of repose.** The angle of repose ( $\theta$ ) provides information about the frictional force among the particles of CSH (in powder form). A fixed funnel method as mentioned in Lachmann *et al.*, and Wells, was followed to measure the angle of repose.<sup>21,22</sup> Briefly, a funnel was fixed on a tripod stand and CSH powder was allowed to fall from the open circumference of the funnel until the apex of the powder heap just met the lower tip of the funnel. The radius ( $r$ , cm) of the base of heap and the height ( $h$ , cm) of the heap was measured to calculate the angle of repose using eqn (1).

$$\tan \theta = \frac{h}{r} \quad (1)$$

**2.4.2. Bulk and tapped density.** An accurately weighed CSH powder ( $W_i$ , 1.0 g) was put in a graduated cylinder to determine the bulk volume ( $V_b$ ). The cylinder was tapped 100 times to get the final tapped volume ( $V_t$ ). The bulk density ( $D_b$ ) and tapped density ( $D_t$ ) were calculated using eqn (2) and (3), respectively.<sup>21</sup>

$$D_b = \frac{W_i}{V_b} \quad (2)$$

$$D_t = \frac{W_i}{V_t} \quad (3)$$

**2.4.3. Hausner ratio and Carr's index.** Hausner ratio ( $H_r$ ) and Carr's index ( $C_i$ ) of any material provides information about the packing arrangement of the particles. The  $H_r$  and  $C_i$  of CSH were determined using eqn (4) and (5), respectively.<sup>21,22</sup>

$$H_r = \frac{D_t}{D_b} \quad (4)$$

$$C_i = \left[ 1 - \frac{D_b}{D_t} \right] \times 100 \quad (5)$$

#### 2.5. Moisture content and loss on drying

The CSH (0.1 g) was dried for 1 h in a vacuum oven at 105 °C. The initial weight ( $W_i$ , before drying) and final weight ( $W_f$ , after drying) of CSH were noted and used to calculate the moisture content (eqn (6)) and loss on drying (eqn (7)).<sup>21</sup>

$$\text{Moisture content}(\%) = \frac{W_i - W_f}{W_f} \times 100 \quad (6)$$

$$\text{Loss on drying}(\%) = \frac{W_i - W_f}{W_i} \times 100 \quad (7)$$

#### 2.6. Stimuli-responsive swelling properties of CSH

The swelling properties of CSH were assessed in DW and buffer of pH 1.2, 6.8, and 7.4. For such an assessment, the tea-bag method as reported by Yoon *et al.*, was used.<sup>23</sup> Accurately weighed amount of dry CSH (100 mg) was placed in each of the four tea bags. The tea bags were sealed and hung in the beakers having swelling media, *i.e.*, DW and buffer of pH 1.2, 6.8, and 7.4 at room temperature. After a pre-defined time interval, the tea bags were taken out from the swelling media and hung to remove excessive swelling media. Later, the tea bags having swollen CSH were weighed and its swelling capacity ( $\text{g g}^{-1}$ ) in every swelling medium was calculated using eqn (8).<sup>24</sup>

$$\text{Swelling capacity of CSH}(\text{g g}^{-1}) = \frac{W_s - W_i - W_e}{W_i} \quad (8)$$

where  $W_s$  is the weight (g) of a wet tea bag having CSH in swollen form,  $W_i$  is the weight (g) of CSH packed in the tea bags for swelling studies, and  $W_e$  is the weight (g) of tea bag before packing CSH in tea-bags.

Additionally, the equilibrium swelling of CSH was also recorded in every swelling medium using the same process as mentioned above. After packing into tea bags, the CSH was allowed to swell for 24 h and the equilibrium swelling capacity was measured using eqn (8).

#### 2.7. Swelling kinetics

The swelling data obtained from the swelling studies of CSH in DW and at pH 1.2, 6.8, and 7.4, was fitted to the eqn (9) for the measurement of normalized degree of swelling ( $Q_t$ ) and eqn (10) for the measurement of the normalized equilibrium degree of swelling ( $Q_e$ ).<sup>14,24</sup> Finally, the values of both  $Q_t$  and  $Q_e$  were fitted to the equation of second-order kinetics (eqn (11)), and the rate at which CSH absorbed swelling media was assessed.

$$Q_t = \frac{W_s - W_d}{W_d} = \frac{W_t}{W_d} \quad (9)$$

$$Q_e = \frac{W_\infty - W_d}{W_d} = \frac{W_e}{W_d} \quad (10)$$

$$\frac{t}{Q_t} = \frac{t}{Q_e} + \frac{1}{kQ_e^2} \quad (11)$$

where,  $W_s$  is the weight (g) of swollen CSH at any time  $t$  (min).  $W_d$  is the initial weight of dry CSH at  $t = 0$ .  $W_t$  is the weight of the swelling medium absorbed by CSH from each swelling medium.  $W_e$  is the weight of the swelling medium retained in CSH at  $t = \infty$ .  $W_\infty$  is the weight of the swollen CSH at time  $t = \infty$ .  $k$  denotes the second-order rate constant.

The values of  $t/Q_t$  were taken along the Y-axis and the values of  $t$  were taken along the X-axis to obtain a straight line plot with



slope  $1/Q_e$  and intercept  $1/kQ_e^2$ . By noting the values of the regression coefficient ( $R^2$ ), the assessment regarding the second-order swelling kinetic for the swelling of CSH was evaluated in every swelling medium.

### 2.8. Effect of electrolytic stress on the swelling of CSH

Besides pH, the swelling potential of any hydrogel system also depends upon the concentrations of salts in the solution and the nature and extent of hydrophilicity of hydrogel. Therefore, the effect of electrolytic stress on the swelling of CSH was also evaluated in this study to establish CSH as a potential candidate for pharmaceutical applications.<sup>25</sup> Aqueous solutions of different concentrations (0.1, 0.2, 0.3, 0.4, 0.5, 1.0, and 1.5 M) of NaCl and KCl were prepared in DW. In every salt solution, the tea-bag containing CSH (100 mg) was immersed for 24 h. After 24 h, the tea bags were taken out from the aqueous salt solution and weighed to calculate the swelling capacity using eqn (8).

### 2.9. On-off switching studies of CSH

The evaluation of CSH as a stimuli-responsive material was determined by conducting the swelling and de-swelling (on-off switching) studies for CSH in buffer of pH 7.4 (swelling medium) *vs.* buffer of pH 1.2 (de-swelling medium), DW (swelling medium) *vs.* ethanol (de-swelling medium), and DW *vs.* 0.9% aqueous solution of NaCl (de-swelling medium) using the tea bag method.<sup>24,26</sup> CSH (100 mg) was taken in a tea bag, sealed, and immersed in the swelling medium, *i.e.*, a buffer of pH 7.4 for 1 h at room temperature. The tea bag was taken out periodically after every 15 min to determine the swelling capacity using eqn (8). After 1 h, the same tea bag enclosed with swollen CSH was transferred to the beaker having a de-swelling medium, *i.e.*, a buffer of pH 1.2, and kept in it for another 1 h. The swelling capacity was calculated using eqn (8) and recorded four consecutive cycles of swelling de-swelling (on-off switching) studies in buffers of pH 7.4 and 1.2 to ascertain the reproducibility of the results. Likewise, swelling de-swelling studies of CSH were also conducted in DW *vs.* ethanol and DW *vs.* normal saline using the above-mentioned procedure.

### 2.10. Haemocompatibility studies of CSH

The interaction of CSH with biological membranes can be evaluated through haemolysis and thrombogenicity. As the CSH is intended to be used in oral DDS, there may be a chance to interact with the inflamed tissues of the gastrointestinal tract. Therefore, it is worth to evaluate the CSH through haemocompatibility studies. Hemocompatibility studies (hemolytic potential and thrombogenicity) of CSH were performed according to the standard procedures of the International Standard Organization (ISO 10993-4, 1999).

**2.10.1. Hemolytic potential.** The haemolytic potential of CSH was determined to evaluate any adverse interaction with the blood following the procedure of the American Society for Testing and Materials (ASTM) and reported elsewhere.<sup>27,28</sup> CSH (500 mg) was soaked at  $37^\circ\text{C} \pm 0.5$  for 24 h in phosphate buffer saline (PBS) and then incubated at  $37^\circ\text{C} \pm 0.5$  for 3 h in the presence of the known concentration of citrate blood. After that,

the mixture was centrifuged at  $10^4$  rpm for 15 min to collect the supernatant. Optical density (OD) of the supernatant was noted through UV-vis spectrophotometer operated at 540 nm. For positive and negative controls, a known concentration of citrate blood and water, and citrate blood and PBS were used, respectively. The haemolytic potential was determined using eqn (12).

$$\text{Haemolytic index}(\%) = \frac{\text{OD of test sample} - \text{OD of}(-)\text{control}}{\text{OD of}(+)\text{control} - \text{OD of}(-)\text{control}} \times 100 \quad (12)$$

**2.10.2. Thrombogenicity.** The thrombogenicity potential of CSH was determined using the gravimetric method.<sup>12,28</sup> Accurately weighed CSH (500 mg) was soaked in PBS for 24 h at  $37^\circ\text{C} \pm 0.5$ . The excessive PBS was decanted and added the citrate blood (2 mL) and  $\text{CaCl}_2$  (0.2 mL, 0.1 M). The mixture was placed unattended for 45 min. DW was added to the mixture to stop the clotting of blood. Formaldehyde (36–38%, 5 mL) was used to fix the clots. These clots were separated, dried, and weighed. For positive and negative control, the same procedure was adopted without CSH and without CSH and blood, respectively. Thrombogenicity was determined using eqn (13).

$$\text{Thrombose}(\%) = \frac{\text{Mass of test sample} - \text{mass of}(-)\text{control}}{\text{Mass of}(+)\text{control} - \text{mass of}(-)\text{control}} \times 100 \quad (13)$$

### 2.11. Development of CSH as sustained release material

**2.11.1. Preparation of CSH and valsartan-based tablets.** To evaluate CSH as a sustained release material for drug delivery applications, the oral tablet formulations of CSH with and without a model drug, *i.e.*, valsartan were prepared according to the wet granulation method. The composition of the tablet constituents used for the preparation of four different oral tablet formulations is given in Table 1. In a pestle and mortar, the CSH, valsartan, and microcrystalline cellulose were thoroughly mixed. Aqueous solution of tragacanth gum (5%, w/v) was prepared and added to the aforesaid mixture as a granulating agent. The prepared damped mixture was kept in an oven under vacuum at  $60^\circ\text{C}$  for 12 h and then sieved by passing through mesh no. 12. The resulting dried granules were first evaluated by pre-compression parameters, such as angle of repose, Carr's index, and Hausner ratio using the procedure described in Section 2.4. Later, the granules were lubricated with magnesium stearate and sent to a compression machine for tablet formation.

#### 2.11.2. Post-compression evaluation

**2.11.2.1. Diameter, thickness, and hardness test.** A hardness tester (Pharma Test, PTB 311E, Germany) was used to measure the hardness, diameter, and thickness of the prepared oral tablet formulations following the procedures mentioned in the USP-NF. For such calculations, ten tablets of each formulation were randomly selected for each measurement, and the mean of the values with standard deviation (SD) are reported here.



**Table 1** Composition (mg) of the constituents of valsartan-loaded CSH-based oral tablet formulations

Composition of oral tablet formulations	CSHF1	CSHF2	CSHF3
CSH	270	370	470
Valsartan	80	80	80
Microcrystalline cellulose	200	100	—
Tragacanth	30	30	30
Magnesium stearate	20	20	20
Total weight	600	600	600

**2.11.2.2. Weight variation test.** From every set of oral tablet formulations, ten tablets were randomly selected and individually weighed. For the calculation of precise weight variation, the test was conducted in triplicate and the average of the values ( $\pm SD$ ) was noted to report the findings.

**2.11.2.3. Friability test.** Ten tablets were randomly picked from every set of tablet formulations and kept in the chamber of the friabilator (Pharma Test, PTF 10E, Germany). The chamber was rotated for 4 min at 25 rpm and then the tablets were removed from the chamber, cleaned from any adhered particles, and weighed accurately. This test was also performed in triplicate and average weight was noted. For the calculation of weight loss in percentage, the difference between the initial ( $w_i$ ) and final weight ( $w_f$ ) of tablets was calculated and divided on the initial weight of the tablets as mentioned in eqn (14).<sup>21</sup>

$$\text{Weight loss}(\%) = \frac{w_i - w_f}{w_i} \times 100 \quad (14)$$

**2.11.2.4. Content uniformity.** Content uniformity is determined to find out the uniform concentration or amount of drug in the DDS. Content uniformity of the valsartan in prepared tablets was determined by following the standard procedure mentioned in the USP-NF. Briefly, ten tablets from each formulation were randomly selected and crushed in a pestle and mortar. The crushed material was weighed and mixed with methanol in a volumetric flask (100 mL) followed by analysis through a UV-vis spectrophotometer (Pharmspec 1700, Shimadzu, Japan) at 250 nm. The content uniformity of the formulations was determined through the calibration curve method.

**2.11.3. Stimuli-responsive swelling behavior of tablets.** The swelling behavior of all of the four prepared tablet formulations of CSH, *i.e.*, CSHF, CSHF1, CSHF2, and CSHF3 in DW, the buffer of pH 1.2, 6.8, and 7.4, and different aqueous solutions of NaCl and KCl were evaluated.<sup>24</sup> Moreover, the swelling and de-swelling behavior of formulation CSHF3 due to its maximum swelling, and maximum contents of CSH were observed in the buffer of pH 7.4 and 1.2, DW and ethanol, and DW and normal saline. The protocol described in sections 2.6, 2.8, and 2.9 was followed for such investigations. In addition, the photographs of the tablet of CSHF3 formulation were captured periodically and the changes that occurred in the shape of the tablet during its swelling were monitored. The SEM images of the tablet of CSHF3 formulation were also recorded using the procedure described in Section 2.3.

**2.11.4. *In vitro* valsartan release study.** The assessment of CSH as a drug delivery carrier for the sustained and targeted delivery of valsartan was evaluated in the buffer of pH 1.2 and 6.8 (900 mL).<sup>29</sup> The dissolution study of the CSHF3 formulation was conducted at  $37 \pm 0.5$  °C and 50 rpm paddle speed using USP Dissolution Apparatus II (Pharma test, Germany). The tablets were placed in their respective dissolution vessels having buffer solutions. The sample (5 mL) was taken out with the help of a pipette after pre-decided time intervals. Every sample was filtered through a 0.45 µm nylon filter and diluted (if required) before recording absorbance on a UV-Vis spectrophotometer at 250 nm. After taking the sample from the dissolution vessels, dissolution vessels were re-filled with the same amount (5 mL) of the respective dissolution media to maintain their level. Moreover, the valsartan release from CSHF3 formulation was also assessed by a pH-change method that mimicked the gastrointestinal tract (GIT) environment, *i.e.*, pH and transit time. Therefore, for 2 h, the valsartan release study was conducted in the buffer of pH 1.2. For the next 6 h, the buffer of pH 6.8 was used for the evaluation of the valsartan release, respectively.

**2.11.5. Valsartan release kinetics.** The release data obtained for the release study of valsartan from CSHF3 was put to the equations of different kinetics models, *i.e.*, zero-order (eqn (15)), first-order (eqn (16)), Hixson–Crowell (eqn (17)), Higuchi (eqn (18)), and Korsmeyer–Peppas (eqn (19)) to study the rate and mechanism of valsartan release. By noting the values of the regression coefficient ( $R^2$ ) from every kinetic model, the “goodness of fit” of the kinetic model to the release data was predicted.

$$Q_t = K_0 t \quad (15)$$

where,  $Q_t$  is the quantity of the valsartan released after time  $t$ . The  $K_0$  is the zero-order rate constant.

$$\log Q = \log Q_0 - \left( \frac{K_1 t}{2.303} \right) \quad (16)$$

where,  $Q$  is the quantity of the valsartan that has to be released after time  $t$ .  $Q_0$  is the initial quantity of the valsartan in the CSH-based matrix tablets.  $K_1$  is the first-order rate constant.<sup>30,31</sup>

$$Q_0^{1/3} - Q_t^{1/3} = -K_{HC} t \quad (17)$$

where,  $Q_0$  is the quantity of valsartan used to prepare tablets.  $Q_t$  is the quantity of valsartan released from CSH-based tablet formulations after time  $t$ .  $K_{HC}$  is a Hixon–Crowell rate constant.<sup>32</sup>

$$Q_t = K_H(t)^{1/2} \quad (18)$$

where,  $Q_t$  is the quantity of valsartan to be released from CSH-based tablet formulations after time  $t$ .  $K_H$  is the Higuchi kinetic model rate constant.<sup>33</sup>

A model-independent approach, *i.e.*, Akaike information criterion as Model Selection Criterion (MSC), was also used for evaluating drug release kinetics using eqn (19).<sup>34</sup>

$$MSC = \ln \left( \frac{\sum_{i=1}^n w_i (Y_{\text{obs}_i} - \bar{Y}_{\text{obs}})^2}{\sum_{i=1}^n w_i (Y_{\text{obs}_i} - Y_{\text{cal}_i})^2} \right) - \frac{2p}{n} \quad (19)$$

where,  $n$  is the number of all data points of valsartan release,  $p$  is the number of parameters,  $w_i$  is the optional weight factor and it will be equal to 1 for the ideal fitting of the model,  $Y_{\text{obs}_i}$  represents the observed value of  $i^{\text{th}}$  data point,  $Y_{\text{cal}_i}$  is the calculated value of  $i^{\text{th}}$  data point, and  $\bar{Y}_{\text{obs}}$  is the mean of observed data points.

**2.11.6. Drug release mechanism.** The mechanism of the release of valsartan from CSH-based tablet formulation was determined by fitting data to the equation of the Korsmeyer-Peppas model (eqn (20)).

$$\frac{M_t}{M_\infty} = k_p t^n \quad (20)$$

where,  $M_t/M_\infty$  is the quantity of valsartan released after time  $t$ ,  $k_p$  is the Korsmeyer-Peppas rate constant, and  $n$  is the diffusion exponent. By knowing the value of  $n$ , the mechanism underlying the release of valsartan can be elucidated. The valsartan can be released through Fickian diffusion ( $n \leq 0.45$ ), non-Fickian diffusion ( $0.45 < n < 0.89$ ), case-II transport ( $n = 0.89$ ), and super case-II transport ( $n \geq 0.89$ ).<sup>35,36</sup>

DDSolver software was used to calculate the release kinetics and release mechanism from CSHF3 formulation.

## 3. Results and discussion

### 3.1. Isolation and characterization of CSH

CSH was isolated using the hot water extraction method. The yield of CSH was 8.2%. Fig. 1(e-h) presented the isolation scheme of CSH and described the physical appearance of chia seeds, swollen chia seeds, swollen chia seeds coated with permitted red food color, and CSH in dry form.

To identify the position of the absorption band as well as major functional groups present in CSH, the FT-IR (KBr pellet method) spectrum of CSH (Fig. 1(a)) was recorded that showed a prominent peak at  $2924 \text{ cm}^{-1}$  due to the presence of hydroxyl functionality of the repeating glycosidic units. A peak at  $2866 \text{ cm}^{-1}$  appeared due to the stretching vibrations of C-H and indicated the presence of  $-\text{CH}$  and  $-\text{CH}_2$  groups in the repeating sugar unit of CSH. Another prominent peak at  $1678 \text{ cm}^{-1}$  appeared because the carbonyl ( $-\text{C}=\text{O}$ ) functional group of carboxylic acid ( $-\text{COOH}$ ) revealed the presence of uronic acid moieties in CSH. It is also noted that some hydroxyls are esterified which appears as an overlapped signal at  $1739 \text{ cm}^{-1}$ .<sup>37</sup> In addition, a broad peak at  $1155\text{--}995 \text{ cm}^{-1}$  appeared because the presence of the C-O-C functional group indicates the glycosidic linkage in the polymeric chains of CSH.<sup>38,39</sup>

The solid-state CP/MAS  $^{13}\text{C}$  NMR spectrum of CSH is shown in Fig. 1(b). A peculiar pattern indicates the presence of signals for pyranose sugars as in other structurally related polysaccharides.<sup>40</sup> Anhydrohexose units appear in the spectrum. The C1 of the sugar units appears at  $104.43 \text{ ppm}$  while C2-6 appears at  $62.43\text{--}89.22 \text{ ppm}$  with overlapped signals. A peak in

the range of  $172.98\text{--}174.20 \text{ ppm}$  is being assigned for the carbonyl groups present in glucuronic acid units of polysaccharide CSH. Also, trace signals of  $\text{CH}_3$  groups of methylated sugar units of CSH appear at  $21.92$  and  $29.98 \text{ ppm}$ .<sup>41</sup>

At  $15 \text{ }^{\circ}\text{C min}^{-1}$  heating rate, the TGA, differential thermogravimetry (DTG), and DSC curves were recorded to evaluate the thermal stability of CSH. The curve shown in Fig. 1(c) represents the TG and Fig. 1(d) represents the DTG curve of CSH. The TG and DTG curves have two regions showing that the CSH thermally decomposes in two steps. Using the TG and DTG curves, the  $T_i$ ,  $T_m$ , and  $T_f$  of CSH were calculated at both the decomposition steps. The  $T_i$ ,  $T_m$  and  $T_f$  at the first decomposition step were  $270$ ,  $310$ , and  $365 \text{ }^{\circ}\text{C}$ , and at the second decomposition step at  $435$ ,  $460$ , and  $475 \text{ }^{\circ}\text{C}$ . These temperatures showed that CSH is a thermally stable moiety that degrades at a slow rate. Its thermal stability is comparable with the already reported polysaccharide-based hydrogel materials extracted from plant seeds.<sup>42,43</sup>

### 3.2. SEM analysis

The CSH was first swelled and then freeze-dried to record its SEM micrographs *via* transverse and longitudinal cross-sections to observe the presence of macroporous channeling on its internal and external surfaces. Moreover, this study provides information about the texture structure of CSH and the arrangements of channels present in the internal structure of the CSH. The SEM images presented in Fig. 2(a)-(f) indicated the presence of uniformly distributed macroporous and interconnected channels on the surface and the interior of the CSH. The histograms shown in the Fig. 2(g) (transverse cross-sections) and Fig. 2(h) (longitudinal cross-sections) indicated the average pore sizes of  $18 \pm 11 \text{ }\mu\text{m}$  and  $23 \pm 15 \text{ }\mu\text{m}$ , respectively of CSH. Hence, due to the presence of these macropores on the surface of CSH, it can be witnessed that the CSH may have an affinity to absorb biological fluids and swell up to a great extent. Therefore, it could be a material of choice for drug delivery applications.

### 3.3. Physical properties of CSH

Table 2 shows the findings of the flow-ability features and physical characteristics of CSH. The angle of repose was  $41.53 \pm 0.5$  which indicated that the CSH has a “passable” flow rate. The  $1.34 \pm 0.11$  and  $25.16 \pm 0.2\%$  are the values of the Hausner ratio and Carr’s index, respectively which witnessed that the CSH has poor ability to flow.<sup>21</sup> Therefore, some necessary parameters are mandatory to enhance the flow rate of CSH before using it for the development of CSH-based tablet formulation. Moreover, it is suggested to adopt necessary procedures when using CSH as an inactive pharmaceutical ingredient, *i.e.*, wet/dry granulation method, use of the appropriate amount of lubricant/glidant, *etc.*

### 3.4. Stimuli-responsive swelling studies

The dynamic swelling behavior of CSH in DW and the buffers of three different pH, *i.e.*, pH 1.2, 6.8, and 7.4 was evaluated to study the potential of CSH as a pH-responsive swellable material for sustained release drug delivery applications. The finding of a swelling study of CSH in all the media is shown in Fig. 3(a).



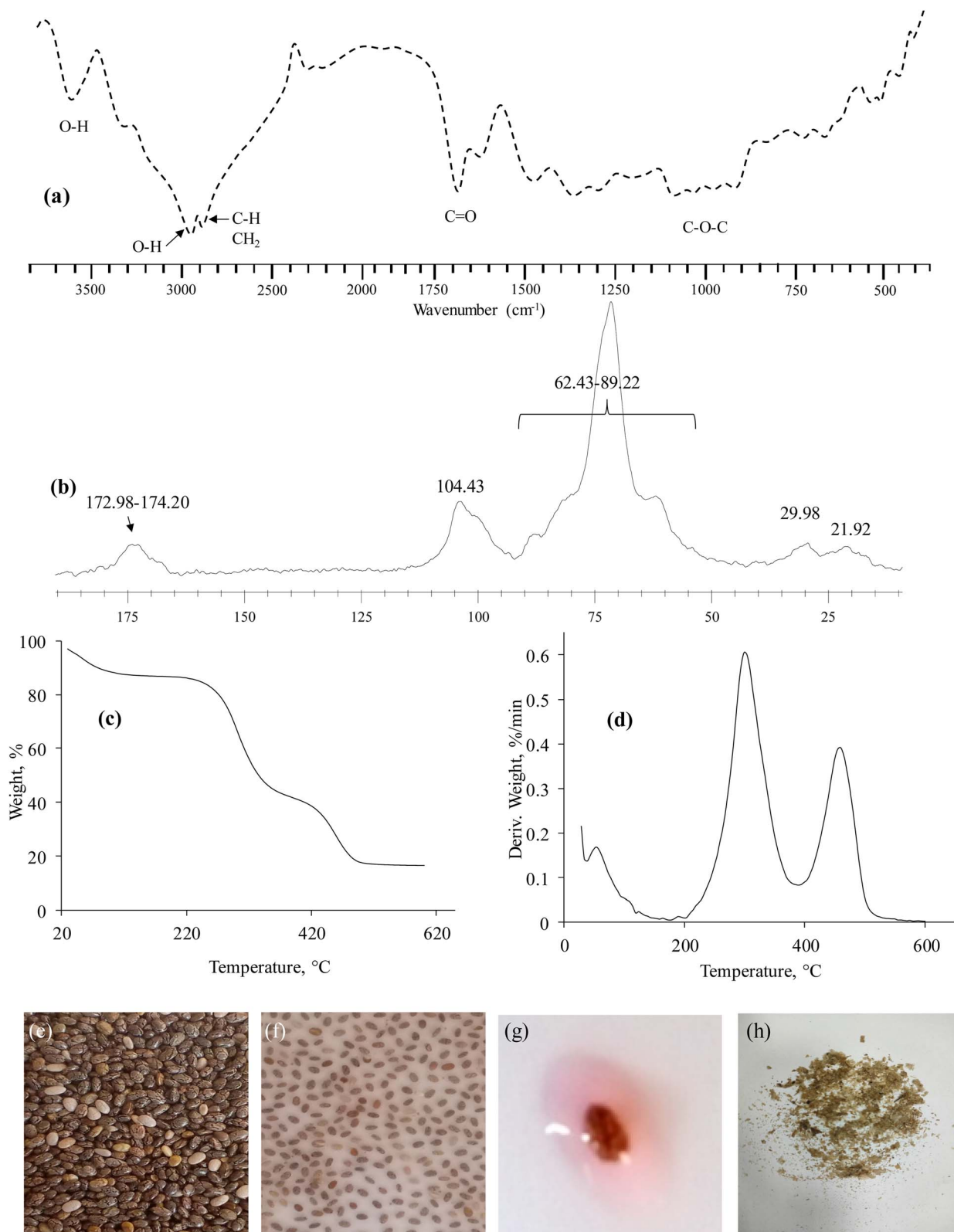


Fig. 1 (a) FTIR spectrum, (b) solid-state CP/MAS <sup>13</sup>C NMR spectrum, (c) TGA curve, (d) DTG curve of CSH, (e) chia seeds, (f) swollen chia seeds, (g) chia seeds coated with permitted red food color, and (h) CSH in dry form.

It can be seen that the CSH swelled maximum in DW and then in buffers of pH 7.4, and 6.8. A very little or insignificant swelling of CSH in the buffer of pH 1.2 was observed. The

reason for the comparatively high swelling of CSH, in the buffer of pH 7.4, is due to the conversion of carboxylic acid groups (COOH) present on the polymer's backbone, *i.e.*, CSH, to the

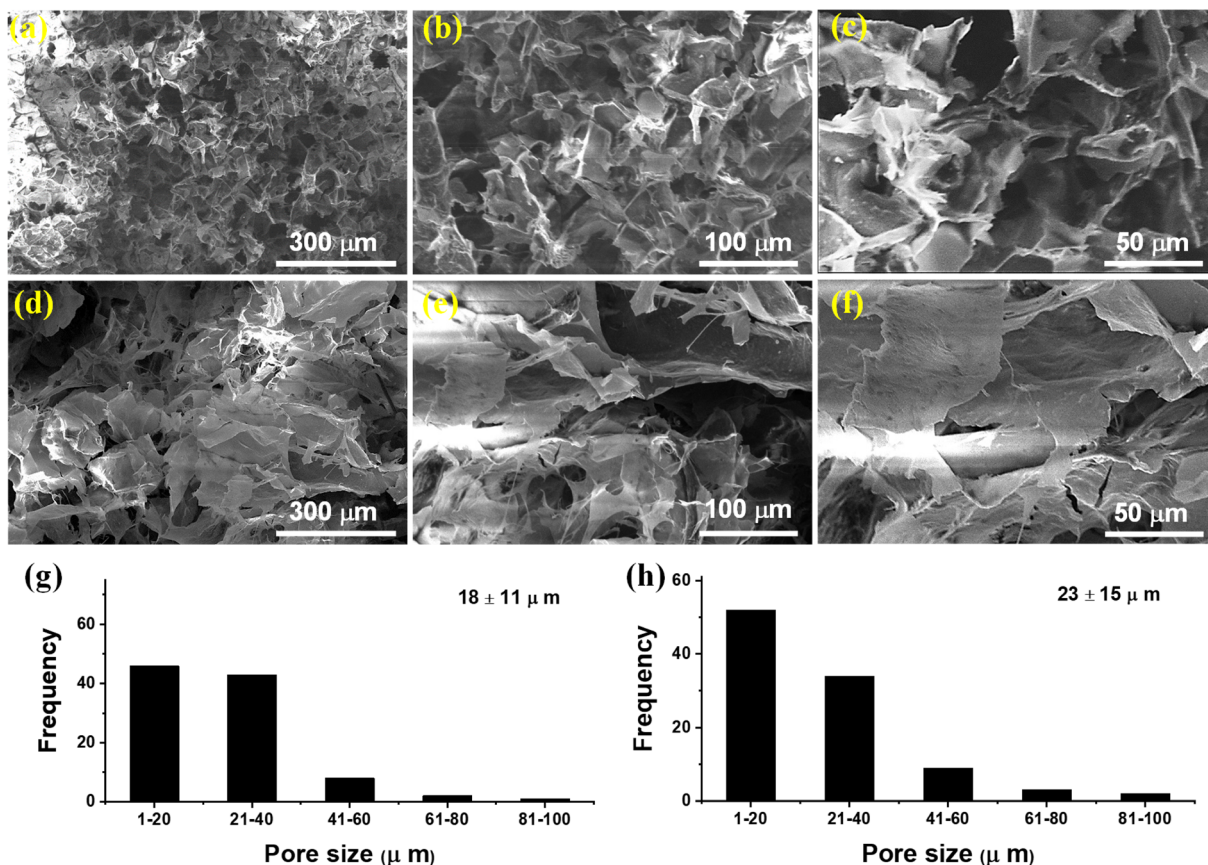


Fig. 2 The SEM images of transverse (a–c) and longitudinal sections (d–f) of swollen then freeze-dried CSH at different magnifications, while (g and h) show the average size distribution of (a–c) and (d–f), respectively.

Table 2 Flow-ability and other physical parameters of CSH

Physical properties	CSH
Moisture content (%)	$6.9 \pm 0.5$
Loss on drying (%)	$6.1 \pm 0.3$
Average particle size ( $\mu\text{m}$ )	$230 \pm 22$
Angle of repose	$41.53 \pm 0.5$
Bulk density ( $\text{g cm}^{-3}$ )	$0.122 \pm 0.031$
Tapped density ( $\text{g cm}^{-3}$ )	$0.163 \pm 0.011$
Carr's index (%)	$25.16 \pm 0.2$
Hausner ratio	$1.34 \pm 0.11$
Swelling capacity ( $\text{g g}^{-1}$ ) after 24 h	$67 \pm 6.4$

carboxylate groups ( $\text{COO}^-$ ).<sup>44</sup> Such a conversion offers electrostatic repulsions between negatively charged carboxylate ions resulting in the relaxation or moving apart of the polymer chains and in turn, CSH swelled.<sup>45</sup> Moreover, the CSH swelling in DW was greater than the buffers of pH 7.4 and 6.8 because the DW has no charge screening effect due to the unavailability of metallic ions, *i.e.*,  $\text{Na}(\text{l})$  and  $\text{K}(\text{l})$  in DW.<sup>46</sup> The absence of these ions imparts less screening effect due to which the CSH swelled more in DW. On the other hand, in the buffer of pH 1.2, the CSH swelled extremely low because of the inability of the ionization of carboxylic acid groups.<sup>44,47</sup> As a result, the polymeric chains remained closely packed with each other and created a hindrance in the entrance of the buffer of pH 1.2. The results

show that the CSH is a pH-sensitive swellable material and could ideally be recommended for drug delivery applications.

### 3.5. Swelling kinetics

Indeed the swelling process of any polymeric material is complex and depends on the rate and extent of the diffusion of the swelling medium to the polymeric material which leads to the swelling as well as erosion of the polymer. The rate of swelling process of the materials from dehydrated to hydrated state is a function of time and can better be explained in terms of second-order swelling kinetics. Therefore, the swelling rate of any material is directly proportional to the ability of the material to absorb the solvent after particular times.<sup>48,49</sup> To know the swelling kinetics, the graph between the  $t/Q_t$  values acquired from the swelling experiments conducted for CSH in all the swelling media was plotted by taking different time intervals along the X-axis and got the straight lines as shown in Fig. 3(b). The values of  $R^2$  were 0.9979, 0.9976, and 0.9981, respectively for DW, the buffers of pH 6.8, and 7.4. These high values of  $R^2$  suggested the best fit of swelling data to the second-order kinetics model equation.<sup>46</sup>

### 3.6. Saline-responsive swelling

The equilibrium swelling (after 24 h) of CSH in different molar solutions of salts ( $\text{NaCl}$  and  $\text{KCl}$ ) was also evaluated to



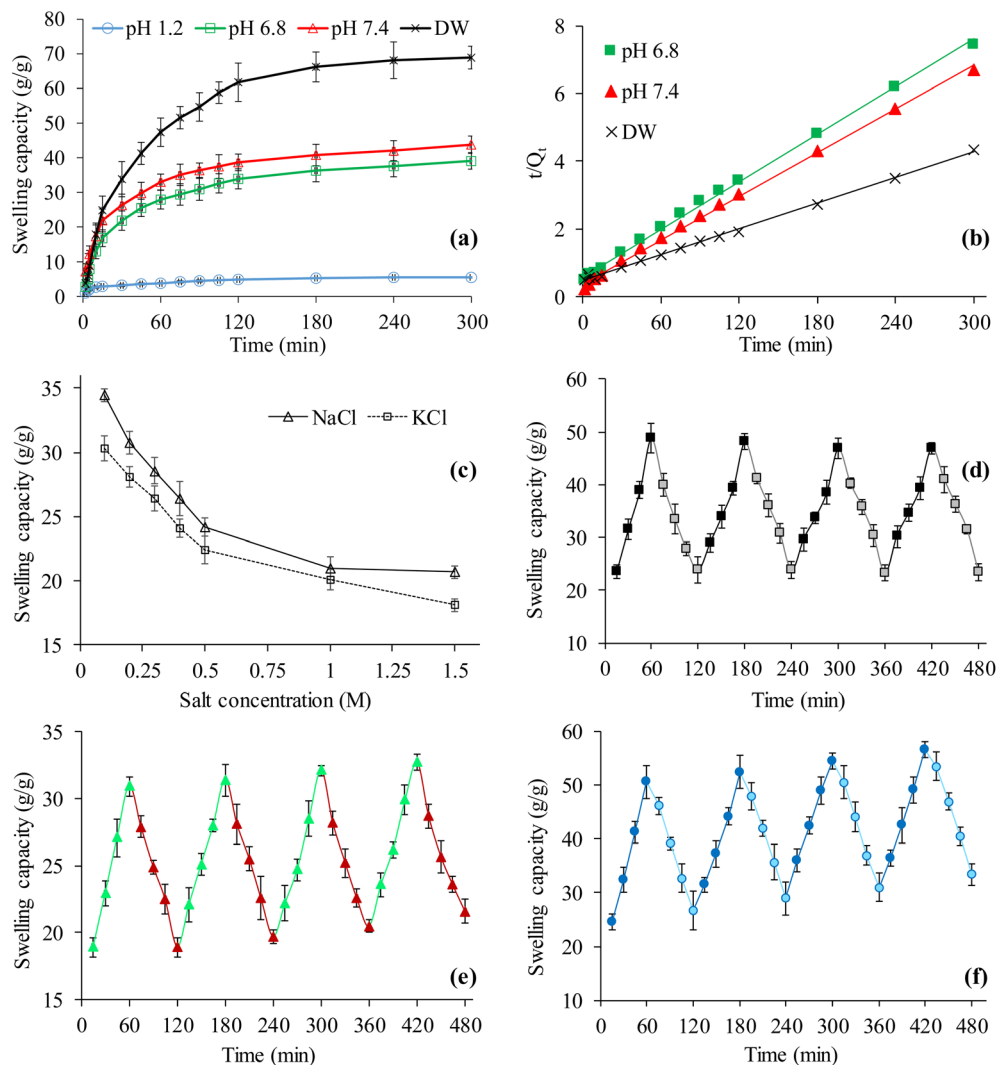


Fig. 3 Stimuli-responsive swelling of CSH in DW and at pH 1.2, 6.8, and 7.4 (a), swelling kinetics of CSH in DW and at pH 6.8, and 7.4 (b), salt-responsive swelling of CSH in NaCl and KCl solutions (c), on–off switching of CSH in DW–ethanol (d), at pH 7.4–1.2 (e), and DW–normal saline (f).

determine the swelling behavior under the influence of salts. The swelling of the CSH was inversely related to the molar concentrations of NaCl and KCl, *i.e.*, upon increasing the molar concentration of the NaCl and KCl in the solutions from 0.1 to 0.5 M, the swelling tends to decrease rapidly. However, the swelling of CSH was negligibly decreased once the molar concentration of the NaCl and KCl in the solutions increased from 0.5 to 2.0 M (Fig. 3(c)).

The abrupt decrease in the swelling of the CSH is due to the strong charge screening effect offered by the Na(*i*) and K(*i*) ions present in the swelling media. Moreover, due to the increase in the concentration of NaCl and KCl in the solutions, there was an increase in the osmotic pressure difference between the salt solutions and the CSH. However, a negligible decrease in the swelling of the CSH from 0.5 to 2.0 M salts concentration is due to the least attractions of the metallic ions with  $-COO^-$  of the CSH.<sup>47,50</sup>

### 3.7. On-off switching properties of CSH

The swelling and de-swelling behavior of CSH was observed in different combinations of the swelling and deswelling media to broaden the applications of CSH. The CSH swelled rapidly in the swelling medium, *i.e.*, DW, and after shifting to the de-swelling medium, *i.e.*, ethanol, it de-swelled (Fig. 3(d)). This swelling and de-swelling behavior of the CSH was due to the difference between the polarities and dielectric constants of the solvents. The dielectric constant of DW is 80.40 and that of ethanol is 24.55. Due to such a high difference between the dielectric constants, the strength of H-bonding between the CSH and ethanol increased during the swelling phase and decreased during the de-swelling phase. Four swelling and de-swelling cycles of CSH in DW and ethanol, respectively were recorded, and similar results were found. Therefore, it can be suggested that habitual and regular users of alcohol-containing beverages should be guided to avoid taking such beverages

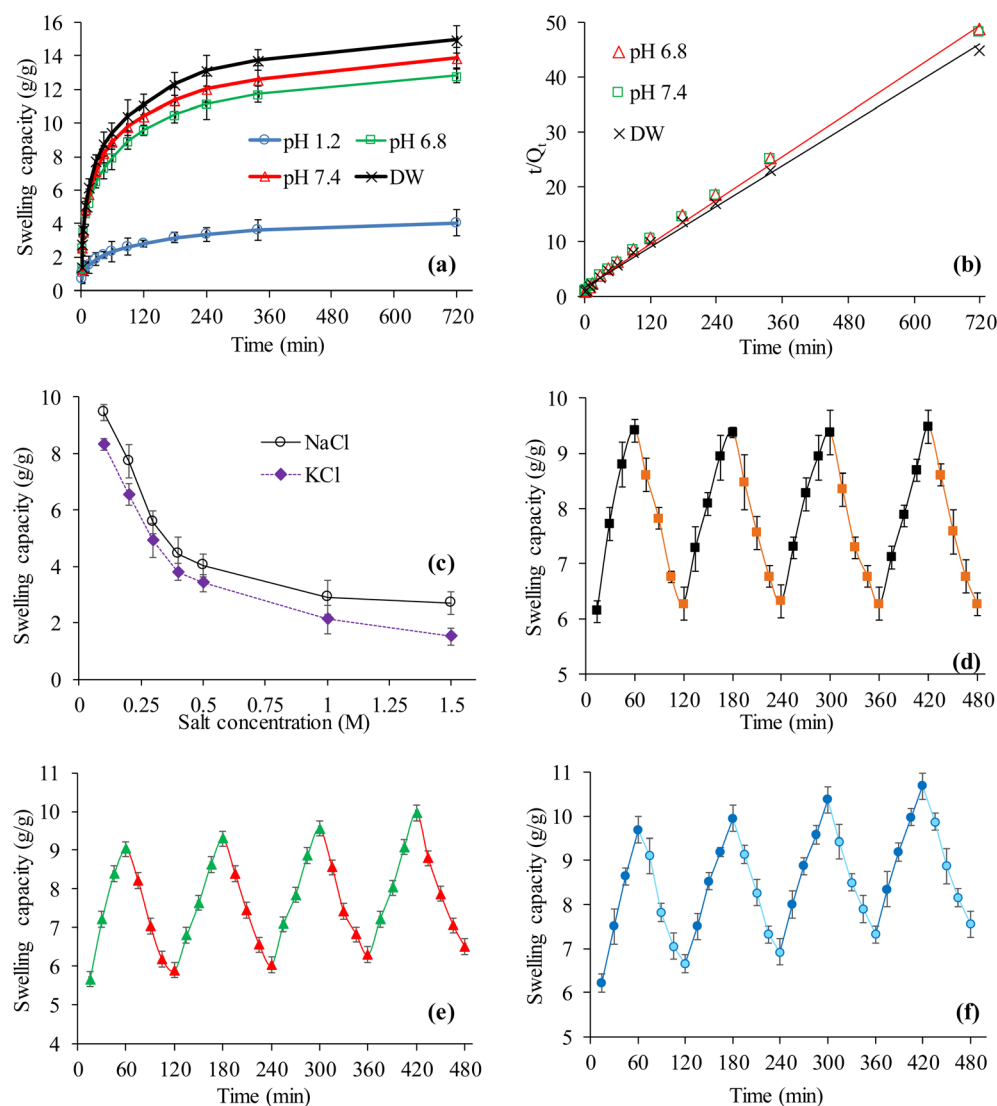


Fig. 4 Stimuli-responsive swelling of CSH-based tablet formulation in DW and at pH 1.2, 6.8, and 7.4 (a), swelling kinetics of CSH-based tablet formulation in DW and at pH 6.8, and 7.4 (b), salt responsive swelling of CSH-based tablet formulation in NaCl and KCl solutions (c), on-off switching of CSH-based tablet formulation in DW and ethanol (d), at pH 7.4 and 1.2 (e), and in DW and normal saline (f).

during medications containing CSH because it may change the pattern of the drug release.<sup>51,52</sup>

The finding of the swelling and de-swelling of CSH at pH 7.4 and 1.2, respectively has been incorporated in the Fig. 3(e). It can be seen that the CSH exhibited rapid swelling in the buffer of pH 7.4 (recorded for 1 h) and after transferring the fully swollen CSH enclosed in a tea bag to the buffer of pH 1.2, it de-swelled completely. This behavior of a CSH in the buffers of pH 7.4 and 1.2 presented its on-off switching properties. The reason for such an increased and decreased swelling of the CSH has already been explained in Section 3.4. Briefly, at pH 7.4, the carboxylic acid groups in the CSH ionized and the electrostatic repulsion between anions started the swelling process. On the other hand, in the buffer of pH 1.2, the re-conversion of  $\text{COO}^-$  to  $\text{COOH}$  started the de-swelling process of CSH. Moreover, the consistency and reproducibility in the on-off switching properties of the CSH at pH 7.4 and 1.2 were studied by recording

four cycles of swelling and de-swelling, and nearly similar behavior was observed.

The rapid swelling of the CSH was observed in the swelling medium, *i.e.*, DW, and de-swelling of the CSH was observed in the de-swelling medium, *i.e.*, normal saline. Such swelling and de-swelling cycles were recorded four times and a similar trend was observed. Results are presented in Fig. 3(f). The reason for the increase and decrease in the swelling of the CSH in the swelling and de-swelling medium has already been described in Section 3.6. Briefly, the charge screening effect decreases the swelling of CSH in normal saline. From these findings, it is obvious, that the CSH is a saline-responsive material and possesses on-off switching behavior.

From the above-mentioned on-off switching studies, it was observed that the CSH did not de-swell completely to the preliminary state or the initial state in the de-swelling media, *i.e.*, the buffer of pH 1.2, and 0.9% NaCl solution, which may be due

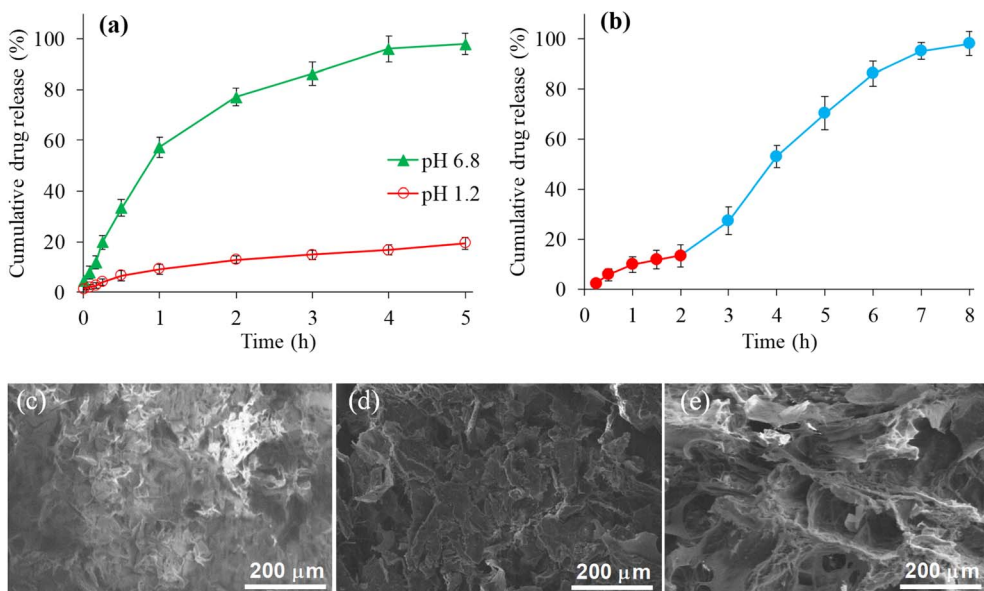


**Fig. 5** Graphical representation of the cumulative drug release study at pH 6.8 and pH 1.2 (a) and physiological pH values of the gastrointestinal tract, *i.e.*, pH 1.2 (red) and pH 6.8 (blue) (b). SEM images of the surface of the tablet (c), the broken surface of the tablet (d), and the surface of the water-swollen then freeze-dried tablet (e).

to the retention of the small amount of swelling media, *i.e.*, the buffer of pH 7.4 and DW in the CSH when shifted to de-swelling media. Furthermore, due to this retention of some amount of swelling media, in every swelling phase, the CSH showed a comparatively high swelling in the next swelling–deswelling cycles. The degree of swelling and deswelling also depends on the functional groups present in the polymer. These groups are mainly responsive to external stimuli and exhibit swelling and deswelling, drug release, and other biological responses.<sup>53,54</sup>

### 3.8. Haemocompatibility studies of CSH

The haemolytic index of the CSH was recorded as  $4.65 \pm 0.08\%$  and the value of thrombosis was calculated as  $89.73 \pm 3.27\%$ . According to the safety standards of the American Society for Testing and Material ASTM F 756-00, a value of haemolytic index of more than 5.0% is considered a haemolytic material and not safe for biomedical applications.<sup>27,28</sup> Similarly, the material having thrombogenicity value less than 100% is referred as non-thrombogenic. Hence, CSH can be considered a safe material for biomedical applications.

### 3.9. Stimuli responsiveness of CSH-based oral tablet formulations

The swelling property of CSHF3 was evaluated in the DW and buffers of the pH 1.2, 6.8, and 7.4. The CSHF3 swelled well in the

DW and buffers of pH 6.8 and 7.4 and negligibly swelled in the buffer of pH 1.2 following a similar pattern as in the case of powdered CSH. However, the swelling of the CSH-based tablets was much less than powdered CSH due to the compression, tight packing, and filling of the interstices of the CSH in the tablet form (Fig. 4(a)).<sup>55</sup> The swelling data obtained from the experimental studies conducted for all of the swelling experiments was fitted to the kinetic equation of second-order and the obtained results are figured out (Fig. 4(b)). The values of  $R^2$  were 0.9996, 0.9963, and 0.9967 for DW, pH 6.8, and 7.4, respectively. This suggested that the swelling of CSHF3 followed second-order swelling kinetics like the powder form of CSH.<sup>48,49,56,57</sup> The effect of salts (NaCl and KCl) on the swelling ability of the CSH-based tablets was evaluated in aqueous solutions of NaCl and KCl. The obtained results are documented in Fig. 4(c). It is revealed that the swelling of the CSHF3 followed the same order as in the case of the CSH powder with a slight decrease in the swelling capacity. The study of on-off switching properties of CSHF3 in DW and ethanol (Fig. 4(d)), DW and normal saline (Fig. 4(e)), and at pH 7.4 and pH 1.2 (Fig. 4(f)) revealed similar trends as in the case of powder CSH. However, it exhibited comparatively less swelling as compared to that of powder CSH due to the compaction of the particles in tablet form.

### 3.10. *In vitro* drug release studies

Fig. 5(a) indicated the sustained release behavior of CSHF3 in the buffer of pH 6.8 for a period of 5 h. Almost 98% drug was

**Table 3** Mathematical data of drug release kinetics modeling from CSHF3

	Zero order			First order			Higuchi			Hixson–Crowell			Korsmeyer–Peppas			
	$R^2$	$K_0$	MSC	$R^2$	$K_1$	MSC	$R^2$	$K_H$	MSC	$R^2$	$K_{HC}$	MSC	$R^2$	$K_{KP}$	MSC	$n$
CSHF3	0.7919	28.95	1.3476	0.9955	0.786	5.1742	0.9746	49.810	3.4504	0.9798	0.215	3.6818	0.9767	48.424	3.3149	0.534

released after 5 h at pH 6.8, whereas, 19.3% drug was released at pH 1.2 (Fig. 5(a)). The drug release from CSHF3 was also studied by changing the pH of the dissolution medium from pH 1.2 to pH 6.8. The obtained release data at all pHs was recorded in terms of percentage plotted against time as shown in Fig. 5(b). The drug release was found negligible (approximately 13%) at pH 1.2 after 2 h. This small amount of drug release can be considered a surface-adherent drug. Upon shifting the same tablet from a dissolution medium of pH 1.2 to a dissolution medium of pH 6.8, the drug release was 98% after a 6 h study at pH 6.8. These investigations indicated that the drug was released from CSHF3 in a sustained fashion and was purely a function of pH.<sup>56-58</sup> Hence, CSH could be a decent choice as a sustained-release material for oral tablet formulation. Fig. 5(c) and (d) show the SEM images of the surface of the tablet, the broken surface of the tablet, and the water-swollen then freeze-dried tablet surface. All images show the microscopic cracks and pores on the surface of the tablet which facilitate the penetration of the swelling as well as the drug release media in the tablet. Moreover, the porous nature of the SSH remained even after the compression in tablet form.

### 3.11. Kinetics and mechanism of drug release studies

The kinetics and mechanism involved in the release of drug from CSHF3 were evaluated by fitting the time-dependent drug release data to the various kinetic models, and the obtained results are displayed in Table 3. To check the best fit of the kinetic model to the drug release data, the values  $R^2$  are very vital. If the values of  $R^2$  are close to the 'one' then the corresponding kinetics model can best describe the drug release finely. To check the mechanism of the drug release data, the values  $n$  are very vital. In this study, the values of  $R^2$  were 0.9955 upon fitting the drug release data to the kinetic equation of the first-order kinetic model. It means that the valsartan release from CSHF3 followed first-order drug release kinetics. The value of  $n$  was 0.534 upon fitting the drug release data to the Korsmaeyer-Peppas kinetic model. This indicated that the release of the drug from CSHF3 followed a non-Fickian diffusion mechanism. Furthermore, the value of MSC was also higher for the first-order mechanism supporting the fact that the drug release followed first-order kinetics.<sup>36</sup>

## 4. Conclusions

The hydrogel from chia seeds (CSH) appeared superporous and superabsorbent. It offers pH-dependent swelling and valsartan release. Drug release studies showed sustained release of valsartan (98%) at pH 6.8 which was in good accord with the swelling pattern of CSH. The swelling of CSH followed 2<sup>nd</sup> order swelling kinetics whereas the drug release was in accord with the non-Fickian mechanism. The negligible swelling at the pH of the stomach (pH 1.2) indicated that the CSH is an ideal material for the preparations of such formulations that can be used to keep the stomach safe from hyperacidity; on the other hand, this way, acid-sensitive drugs can be kept safe from the harsh environment of the stomach as well. The CSH exhibited

exceptional on/off switching behavior due to which it can be utilized for designing benign and intellectual DDSs. Moreover, the haemocompatibility of the CSH can broaden the horizon of its biomedical application. The studies regarding surface morphology revealed the porous nature of CSH which also indicates it as an admirable smart material for pharmaceutical applications. Such superporous (15–18  $\mu$ m), super absorbent, pH-sensitive polysaccharide materials have a promising future for developing intelligent drug delivery systems on a commercial scale.

## Data availability

All data generated or analyzed during this study are included in this published article.

## Author contributions

Maria Khatoon: investigation, writing – original draft. Arshad Ali: methodology, writing – original draft. Muhammad Ajaz Hussain: conceptualization, supervision, project administration, writing – review & editing. Muhammad Tahir Haseeb: validation, writing – review & editing. Muhammad Sher: formal analysis, resources. Omar A. Alsaidan: resources, project administration. Gulzar Muhammad: formal analysis, resources. Syed Zajif Hussain: investigation, formal analysis, validation. Irshad Hussain: validation, resources. Syed Nasir Abbas Bukhari: investigation, conceptualization.

## Conflicts of interest

There are no conflicts to declare.

## Acknowledgements

The authors extend their appreciation to the Deputyship for Research & Innovation, Ministry of Education in Saudi Arabia for funding this research work through the project number 223202.

## References

- 1 M. Samateh, N. Pottackal, S. Manafirasi, A. Vidyasagar, C. Maldarelli and G. John, *Sci. Rep.*, 2018, **8**, 7315.
- 2 R. Ayerza, *J. Am. Oil Chem. Soc.*, 1995, **72**, 1079–1081.
- 3 Z. Din, M. Alam, H. Ullah, D. Shi, B. Xu, H. Li and C. Xiao, *Food Hydrocolloids Health*, 2021, **1**, 100010.
- 4 M. de la Paz Salgado-Cruz, G. Calderón-Domínguez, J. Chanona-Pérez, R. R. Farrera-Rebollo, J. V. Méndez-Méndez and M. Díaz-Ramírez, *Ind. Crops Prod.*, 2013, **51**, 453–462.
- 5 K. Y. Lin, J. R. Daniel and R. L. Whistler, *Carbohydr. Polym.*, 1994, **23**, 13–18.
- 6 Y. P. Timilsena, R. Adhikari, S. Kasapis and B. Adhikari, *Carbohydr. Polym.*, 2016, **136**, 128–136.
- 7 Y. Guterman and S. Shem-Tov, *J. Arid Environ.*, 1997, **35**, 695–705.

8 G. Avila-De La Rosa, J. Alvarez-Ramirez, E. J. Vernon-Carter, H. Carrillo-Navas and C. Pérez-Alonso, *Food Hydrocolloids*, 2015, **49**, 200–207.

9 M. I. Capitani, V. Y. Ixtaina, S. M. Nolasco and M. C. Tomás, *J. Sci. Food Agric.*, 2013, **93**, 3856–3862.

10 M. I. Capitani, V. Spotorno, S. M. Nolasco and M. C. Tomás, *LWT-Food Sci. Technol.*, 2012, **45**, 94–102.

11 G. Ferraro, E. Fratini, P. Sacco, F. Asaro, F. Cuomo, I. Donati and F. Lopez, *Food Hydrocolloids*, 2022, **129**, 107614.

12 A. Ali, M. A. Hussain, M. T. Haseeb, U. Ashraf, M. Farid-Ul-Haq, T. Tabassum, G. Muhammad, A. Abbas and J. Braz, *Chem. Sci.*, 2023, **34**, 906–917.

13 M. Farid-ul-Haq, M. T. Haseeb, M. A. Hussain, M. U. Ashraf, M. Naeem-ul-Hassan, S. Z. Hussain and I. Hussain, *J. Drug Delivery Sci. Technol.*, 2020, **58**, 101795.

14 M. U. Ashraf, M. A. Hussain, G. Muhammad, M. T. Haseeb, S. Bashir, S. Z. Hussain and I. Hussain, *Int. J. Biol. Macromol.*, 2017, **95**, 138–144.

15 M. A. Hussain, G. Muhammad, I. Jantan and S. N. A. Bukhari, *Polym. Rev.*, 2016, **56**, 1–30.

16 B. Liu and K. Chen, *Gels*, 2024, **10**, 262.

17 J. Li and D. Mooney, *Nat. Rev. Mater.*, 2016, **1**, 16071.

18 P. Kesharwani, A. Bisht, A. Alexander, V. Dave and S. Sharma, *J. Drug Delivery Sci. Technol.*, 2021, **66**, 102914.

19 R. Rendón-Villalobos, A. Ortíz-Sánchez, J. Solorza-Feria and C. A. Trujillo-Hernández, *Czech J. Food Sci.*, 2012, **30**, 118–125.

20 I. Salahshoori, Z. Ramezani, I. Cacciotti, A. Yazdanbakhsh, M. K. Hossain and M. Hassanzadeganroudsari, *J. Mol. Liq.*, 2021, **344**, 117890.

21 L. Lachmann, H. A. Liberman and J. L. Kanig, *Theory and Practice of Industrial Pharmacy*, Lea and Febiger, Philadelphia, 3rd edn, 1987.

22 J. I. Well and M. E. Aulton, in *Pharmaceutics; the Science of Dosage Form Design*, ed. M. E. Aulton, Churchill Livingstone, Edinburgh, 1988, pp. 223–253.

23 S. W. Yoon, D. J. Chung and J. H. Kim, *J. Appl. Polym. Sci.*, 2003, **90**, 3741–3746.

24 J. Irfan, A. Ali, M. A. Hussain, M. T. Haseeb, M. Naeem-ul-Hassan and S. Z. Hussain, *RSC Adv.*, 2024, **14**, 8018.

25 Y. Wang, G. He, Z. Li, J. Hua, M. Wu, J. Gong, J. Zhang, L. T. Ban and L. Huang, *Polymers*, 2018, **10**, 112.

26 E. S. Dragan and D. F. Apopei, *Carbohydr. Polym.*, 2013, **92**, 23–32.

27 American Society for Testing and Material ASTM F 756-00: Standard Practices for Assessment of Haemolytic Properties of Material, Philadelphia, 2000.

28 N. Thakur and B. Singh, *Int. J. Biol. Macromol.*, 2024, **274**, 133527.

29 A. Ali, M. A. Hussain, M. T. Haseeb, S. N. A. Bukhari, G. Muhammad, F. A. Sheikh, M. Farid-ul-Haq and N. Ahmad, *Curr. Drug Delivery*, 2023, **20**, 292–305.

30 M. Gibaldi and S. Feldman, *J. Pharm. Sci.*, 1967, **56**, 1238–1242.

31 J. G. Wagner, *J. Pharm. Sci.*, 1969, **58**, 1253–1257.

32 A. W. Hixson and J. H. Crowell, *Ind. Eng. Chem.*, 1931, **23**, 1160–1168.

33 T. Higuchi, *J. Pharm. Sci.*, 1963, **52**, 1145–1149.

34 M. S. Iqbal, J. Akbar, M. A. Hussain, S. Saghir and M. Sher, *Carbohydr. Polym.*, 2011, **83**, 1218–1225.

35 R. W. Korsmeyer, R. Gurny, E. Doelker, P. Buri and N. A. Peppas, *Int. J. Pharm.*, 1983, **15**, 25–35.

36 P. I. Ritger and N. A. Peppas, *J. Controlled Release*, 1987, **5**, 37–42.

37 J. C. Boulet, P. Williams and T. Doco, *Carbohydr. Polym.*, 2007, **69**, 79–85.

38 M. Kacurakova, P. Capek, V. Sasinkova, N. Wellner and A. Ebringerova, *Carbohydr. Polym.*, 2000, **43**, 195–203.

39 J. C. Boulet, P. Williams and T. Doco, *Carbohydr. Polym.*, 2007, **69**, 79–85.

40 K. Y. Qian, S. W. Cui, J. Nikiforuk and H. D. Goff, *Carbohydr. Res.*, 2012, **362**, 47–55.

41 T. H. Emaga, N. Rabetafika, C. S. Blecker and M. Paquot, *Biotechnol., Agron., Soc. Environ.*, 2012, **16**, 139–147.

42 M. Farid-ul-Haq, M. Amin, M. A. Hussain, M. Sher, T. A. Khan, F. Kausar and H. M. A. Amin, *Int. J. Polym. Anal. Charact.*, 2020, **25**, 529–538.

43 A. Ali, M. A. Hussain, A. Abbas, T. A. Khan, G. Muhammad, M. T. Haseeb and I. Azhar, *Cellul. Chem. Technol.*, 2022, **56**, 239–250.

44 M. Rizwan, R. Yahya, A. Hassan, M. Yar, A. D. Azzahari, V. Selvanathan, F. Sonsudin and C. N. Abouloula, *Polymers*, 2017, **9**, 137.

45 M. Chen, Z. Ni, Y. Shen, G. Xiang and L. Xu, *Colloids Surf., A*, 2020, **602**, 125133.

46 E. Diez-Pena, I. Quijada-Garrido and J. M. Barrales-Rienda, *Macromolecules*, 2002, **35**, 8882–8888.

47 N. A. Peppas and A. G. Mikes, *Hydrogels in Medicine and Pharmacy*, CRC Press, Boca Raton, FL, 1986, vol. 1.

48 H. Schott, *J. Macromol. Sci., Part B: Phys.*, 1992, **31**, 1–9.

49 H. Schott, *J. Pharm. Sci.*, 1992, **81**, 467–470.

50 M. K. A. Pourjavadi, *Eur. Polym. J.*, 2007, **43**, 877–889.

51 M. Walden, F. A. Nicholls and K. J. Smith, *Drug Dev. Ind. Pharm.*, 2007, **33**, 1101–1111.

52 V. Friuli, G. Bruni, G. Musitelli, U. Conte and L. Maggi, *J. Pharm. Sci.*, 2018, **107**, 507–511.

53 Z. Yuan, J. Ding, Y. Zhang, B. Huang, Z. Song, X. Meng, X. Ma, X. Gong, Z. Huang, S. Ma, S. Xiang and W. Xu, *Eur. Polym. J.*, 2022, **177**, 111473.

54 A. Raza, T. Rasheed, F. Nabeel, U. Hayat, M. Bilal and H. M. N. Iqbal, *Molecules*, 2019, **24**, 1117.

55 R. S. Harland, A. Gazzaniga, M. E. Sangalli, P. Colombo and N. A. Peppas, *Pharm. Res.*, 1988, **5**, 488–494.

56 B. A. Lodhi, M. A. Hussain, M. U. Ashraf, M. T. Haseeb, G. Muhammad, M. Farid-ul-Haq and M. Naeem-ul-Hassan, *Ind. Crops Prod.*, 2020, **155**, 112780.

57 G. Muhammad, M. T. Haseeb, M. A. Hussain, M. U. Ashraf, M. Farid-ul-Haq and M. Zaman, *Drug Dev. Ind. Pharm.*, 2020, **46**, 122–134.

58 M. A. Hussain and M. T. Haseeb, *Cellul. Chem. Technol.*, 2024, **58**, 249–258.

